

The Study of Longitudinal Joint with Tensile Grip Connection in Highway Bridges

교축방향 인장이음에 관한 연구

서성탁*
Seung-Tag Seo*

<Abstract>

합성상판을 시공하는 경우 교축방향에 분할된 저강판을 접합 일체화해야 한다. 본 논문에서는 강·콘크리트 합성상판을 대상으로 3종류의 배력철근 방향 이음구조를 제안하며, 보 공시체에 의한 정적·정점피로 실험한다. 그 결과 보의 피로실험 결과 저강판 혹은 고력볼트가 피로파단 하였으며, 3차원 FEM해석에 이음부의 휨 강성도 및 피로강도에 대해서 해석적으로 검토된다.

Key Words: composite slab, tensile grip connection, fatigue test, high-strength bolt, bending moment

1. Introduction

Recently, steel-concrete composite deck slabs have been widely used for highway bridge decks. In the construction of composite decks, it is necessary to join two adjacent blocked bottom plates in the longitudinal direction to form one united plate. To achieve the performance required of the connection in the longitudinal direction, it is necessary to fully transmit both bending moment and shearing force and to simplify the connection system. In this paper, three types of longitudinal joint that use tensile grip connection for Robinson-type composite deck slabs are proposed. Static and fatigue bending tests are carried out by using beam specimens to investigate the joint stiffness and distribution of bending moment. A typical Robinson-type composite deck

slab is shown in Fig.1. The stress and deformation of the tensile grip connection with high-strength bolts are also discussed by using three-dimensional elasto-plastic FEM analysis.

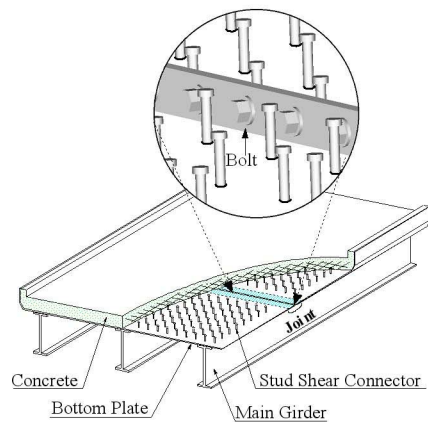


Fig.1 Robinson-type Composite Deck Slabs

* Member, Lecturer, Dept. of Civil Engineering, KyungIl, Korea
E-mail: seosungtag@yumail.ac.kr

2. Outline of Test and Analysis

2.1 Joint Structure

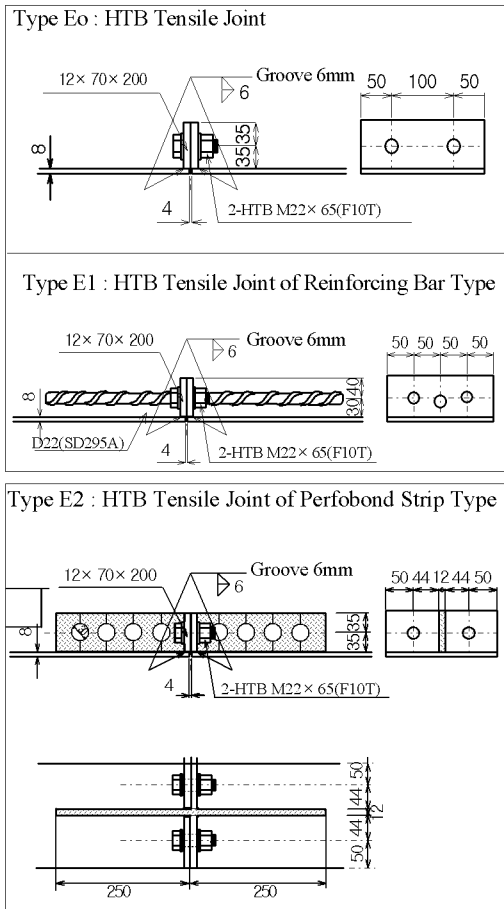


Fig. 2 Joint Structures

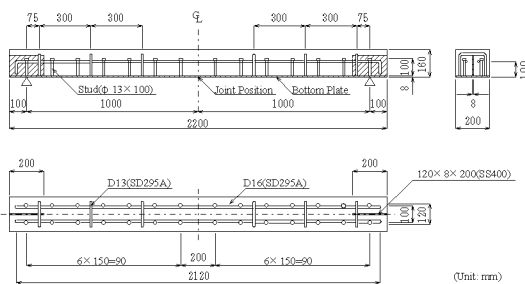


Fig. 3 Dimensions of Specimen

As shown in Fig.2, three types of longitudinal joint in the middle span of deck slabs are proposed. Type Eo is a tensile grip connection with high-strength bolts. Types E1 and E2 are tensile grip connections reinforced by reinforcing bar and perfobond strip,

respectively. A specimen without joint was also tested for comparison with the specimens with joint. These types of joint were selected on basis of the previous test results of the authors^{1),2),3)}. Fig.3 illustrates the detailed dimensions of the test beams which were used in fatigue tests as well as static tests. All specimens are composite beams with stud shear connectors and have the same sections excluding the joint structure in the middle span.

2.2 Test Procedure

All specimens were tested on simply supported beams under one and two-concentrated loadings. Photo.1 shows the set-up of the specimen. In the fatigue test, the load amplitude of three stages presented in Table 1 was set to the tensile stress amplitude of the bottom steel plate⁴⁾. The loading cycle from loading stage 1 to loading stage 3 was performed until failure occurred after 500,000 to 1,000,000 cycles. The fatigue tests were performed under load control with a servo-type fatigue machine Servo Pulser EHF-30. In the static test, the load was increased gradually with an increment of 4.9 kN after three repetitions up to the maximum load in the fatigue test. At each loading stage, deflection, strain and separation width of the joint were measured. After failure, the ultimate load was recorded and the failure mode of each specimen was observed.

2.3 Analytical Procedure

The three-dimensional elastic-plastic FEM analysis was carried out by using commercial software, LUSAS Ver 13.2. The strength and deflections of the joint were investigated by three-dimensional elasto-plastic analysis. Fig.4 shows the F.E mesh, in which the solid element with eight-node isoparametric element was used to model the bottom plate, concrete and the end plate. The bar element was used to model the reinforcing bar. In the tensile grip connection, the bolt was modeled by the solid element to simulate the actual structure. The head of the bolt was assumed to be a rigid connection with the end plate. It was assumed that the adhesion of concrete and the bottom plate was full composite.



Photo.1 Set up of Specimen

Table 1. Loading Procedures

Loading Stage	Maximum Load	
	Two Point	One Point
1	20.5 kN	15.6 kN
2	36.2 kN	27.4 kN
3	58.8 kN	44.1 kN

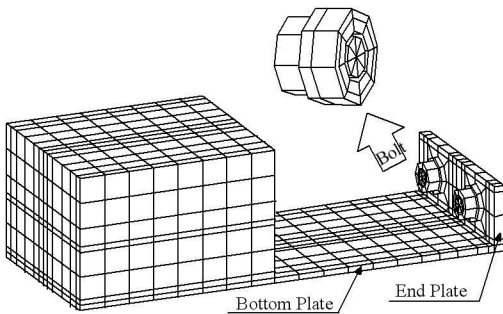


Fig.4 F.E Mesh for Specimen

3. Test Results and Discussion

Table 2 presents the results of the fatigue and static tests. The failure mode in the fatigue test is fatigue failure of the bottom plate or of the high-strength bolt. Photo.2 shows the fatigue failure mode of the bottom plate. This is in contrast to the bending crush of concrete in the compressive zone for static tests. The calculated value of the ultimate load is based on the RC theory.

3.1 Deflection of the Beam

Fig.5 shows a few examples of maximum and

residual deflections at the midspan of the beam in the fatigue test. The residual deflection hardly occurred even at the load level (58.8 kN) which corresponded to three times the design bending moment by live load.

Table 2. Summary of the Experimental Results

Specimen		Loading Stage	Maximum	Cycles(N)	
Type Eo	Static	No.1	Experimental Value: 98.8 kN Calculated Value: 106.7 kN		
		Fatigue (Two Point)	No.2	(2)	36.2 kN
	No.3		(1)	20.5 kN	1,000,000
			(2)	36.2 kN	559,000
	No.4		(2)	36.2 kN	942,000
	No.5		(1)	20.5 kN	500,000
		(2)	36.2 kN	510,000	
	Fatigue (One Point)	No.6	(1)	15.6 kN	50,000
			(2)	27.4 kN	910,000
		No.7	(1)	15.6 kN	500,000
(2)			27.4 kN	890,000	
Type E1	Static	No.1	Experimental Value: 116.3 kN Calculated Value: 117.1 kN		
		Fatigue (Two Point)	No.2	(1)	20.5 kN
	(2)		36.2 kN	1,000,000	
	(3)		58.8 kN	1,200,000	
	Fatigue (One Point)	No.3	(1)	15.6 kN	500,000
			(2)	27.4 kN	1,000,000
			(3)	44.1 kN	200,000
		No.4	(1)	15.6 kN	500,000
			(2)	27.4 kN	1,000,000
			(3)	44.1 kN	150,000
Type E2	Static	No.1	Experimental Value: 115.6 kN Calculated Value: 117.8 kN		
		Fatigue (Two Point)	No.2	(1)	20.5 kN
	(2)		36.2 kN	1,000,000	
	(3)		58.8 kN	28,000	
	Fatigue (One Point)	No.3	(1)	15.6 kN	500,000
			(2)	27.4 kN	1,000,000
			(3)	44.1 kN	300,000
		No.4	(1)	15.6 kN	500,000
			(2)	27.4 kN	1,000,000
			(3)	44.1 kN	90,000
Type A	Static	No.1	Experimental Value: 157.3 kN Calculated Value: 133.3 kN		

From Fig.5, it may be concluded that the tensile grip joints Types Eo, E1 and E2 have sufficient fatigue durability. Fig.6 shows the relation between the stress amplitude and the width of separation amplitude at the bottom plate. All types show elastic behavior. As a result, the stiffness of the connection

was influenced by the bending moment. Fig. 7 shows the deflection curves at the midspan in the static tests. Both experimental and analytical values were almost linear up to twice the design bending moment (load 36.2 kN). Fig. 8 shows the transformation image of the bottom plate and the end plate by the FEM analysis. Negative bending stress partially occurred at the midspan of the bottom plate. Fatigue failure of the bottom plate was caused by the repetition of these local negative stresses under a positive stress all over the span.

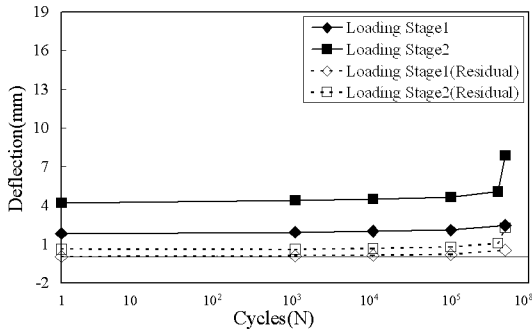


Fig. 5 (a) Deflection-Cycles Relationship (Eo, No. 1)

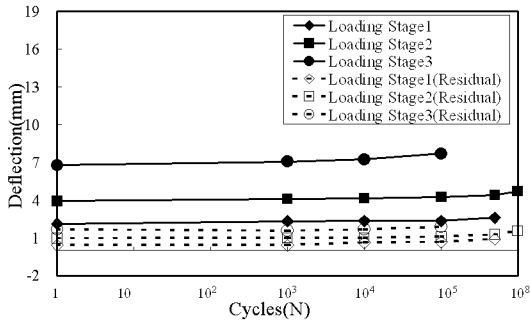


Fig. 5 (b) Deflection-Cycles Relationship (E1, No. 1)

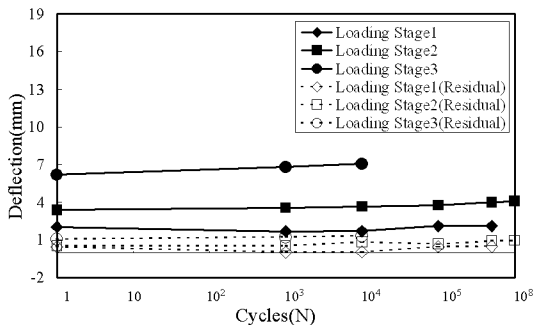


Fig. 5 (c) Deflection-Cycles Relationship (E2, No. 1)

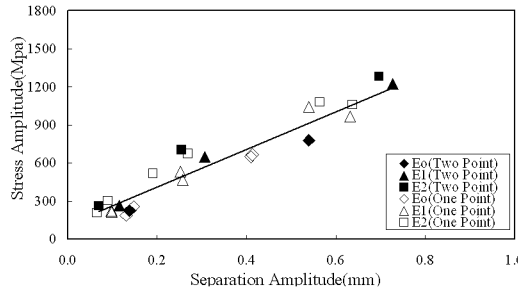


Fig. 6 Stress-Separation Amplitude Relationship for the bottom plate

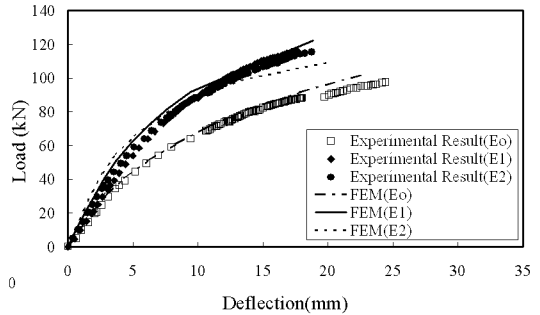


Fig. 7 Load-Deflection Relationship (Static)

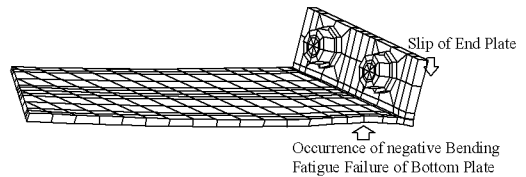


Fig. 8 Fatigue Failure Mode by F.E.M

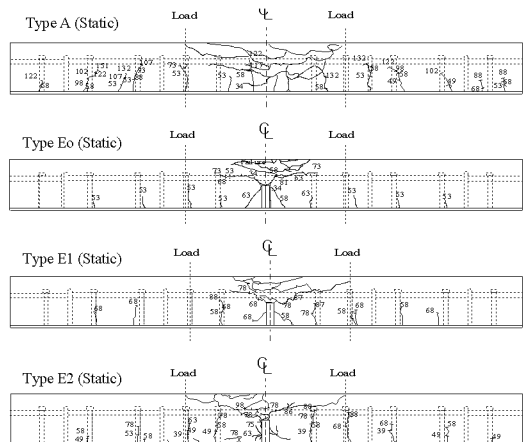


Fig. 9 Crack Distributions of Specimens

3.2 Crack Distribution

Fig.9 shows the crack distribution on the side of each specimen after failure. For Type Eo, the crack developed from the upper surface of the end plate to the bottom plate. The cracks were also concentrated in the joint of the end plate and concrete. It seems that partial shearing force acted due to the L shape of the steel. The cracks of Types E1 and E2 were concentrated on the connections compared with Type A, but they showed a better crack distribution than Type Eo because of the effect of the additional reinforcements of the joint.

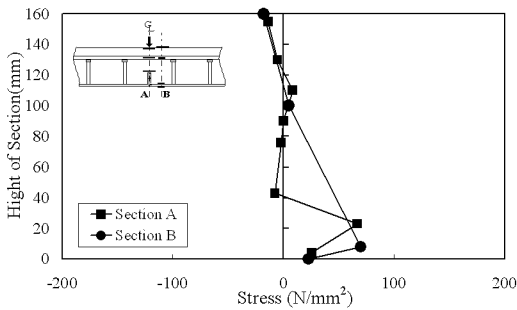


Fig. 10 (a) Stress Distribution of End Plate (Eo, No.3)

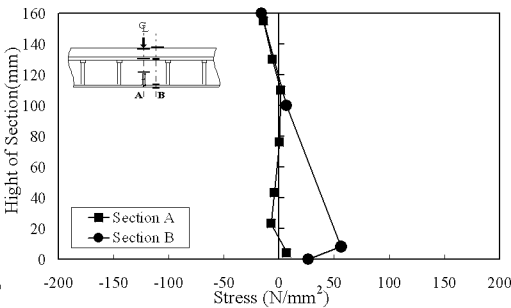


Fig. 10 (b) Stress Distribution of End Plate (E1, No.3)

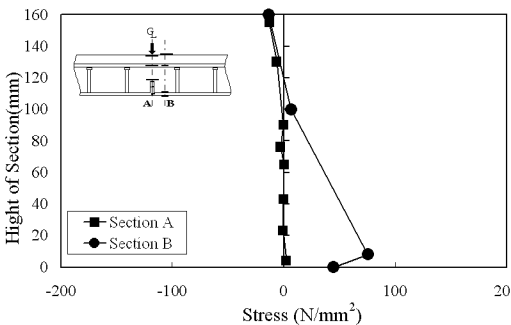


Fig. 10 (c) Stress Distribution of End Plate (E2, No.3)

3.3 Stress Distribution of the End Plate

Fig.10 shows the stress distribution of the end plate and section 5 cm from the central section, which was obtained at loading stage 2 in the fatigue test. The compressive stress occurred at the bolt position and the deformation of the end plate was caused by the tension force of the bottom plate. On the other hand, the stress did not concentrate on the cross section of the center span for Types E1 and E2. The stress was shared among the reinforcing bar, perfbond strip and bolt, respectively. As a result, stress concentration might be avoided sufficiently in a discontinuous section.

3.4 Curvature in the Joint

To examine the decrease of flexural stiffness as a result of the separation of the joint section, the relation between bending moment (M) and curvature (ϕ) is presented in Fig.11. The curve was linear in the initial loading stage. But, flexural stiffness rapidly decreased when the crack occurred in the contact side of the end plate and concrete. Comparing the flexural stiffness of each joint, Type A was the largest, followed by Types E1 and E2. Compared with Type Eo, the improved joint structure was clearly proved to enhance the joint stiffness.

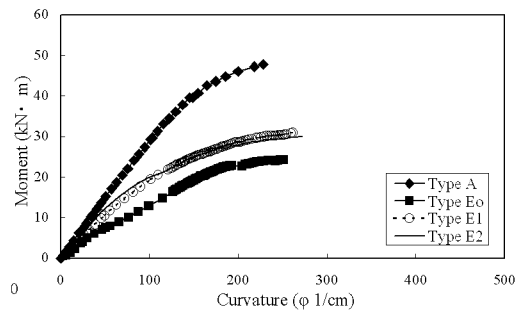


Fig. 11 Moment-Curvature relationships

3.5 Assessment of S-N Curve and Joint Performance

The S-N curve in the bottom plate of the tested joint is shown in Fig.12. The equivalent stress range $\Delta\sigma_e$

given below gives equivalent fatigue damage for the same number of stress cycles as the variable amplitude stresses. The equivalent stress range equation is as follows:

$$\Delta\sigma_e = \left[\sum_{i=1} \left\{ (\Delta\sigma_i)^3 (N_i / N_e) \right\} \right]^{1/3} \quad (1)$$

where $\Delta\sigma_e$ is equivalent stress range, σ_i is stress range in the level i , N_i is fatigue life under stress range $\Delta\sigma_i$ and N_e is total fatigue life. Here, the straight line is the allowable stress range provided by fatigue design recommendations for steel structures⁵⁾, and the fatigue strength category of the bottom plate in the joint part is distributed between level F and H. From the above results, the static and fatigue tests are analyzed in detail. The joint performance is assessed in terms of durability and construction. The result of the fatigue test showed no remarkable difference between one and two-concentrated loading tests. The cracks in the bottom plate and concrete occurred due to bending moment. As for improved joint structures E1 and E2, fatigue failure occurred in loading stage 3. The decrease of joint performance was not caused by the separation of the bottom plate. Thus, it is considered that Types E1 and E2 have the same joint performance as the welding joint of the end plate. In the static test, the maximum load of each type has three times or higher safety than the design load. As for improved joint structures, the distribution of the crack was improved more than Type Eo. The construction is also good because all the joint work can be done on the floor. Especially, Type E1 is very practical because it is a simple structure and has the same joint performance as Type E2.

5. Conclusions

In conclusion, the followings can be summarized :

- (1) For the fatigue test of Type Eo, the bottom plate failed by separation of the end plate at loading stage 2.
- (2) For improved joint structures Types E1 and E2, the joint performance did not decrease even for fatigue failure of the bottom plate. The joint structures have a safety excess of three times or

more the maximum design load.

- (3) The failure pattern in the fatigue test was fatigue of the bottom plate in the vicinity of the welding point. The fatigue strength was distributed between level F and H of JSSC.

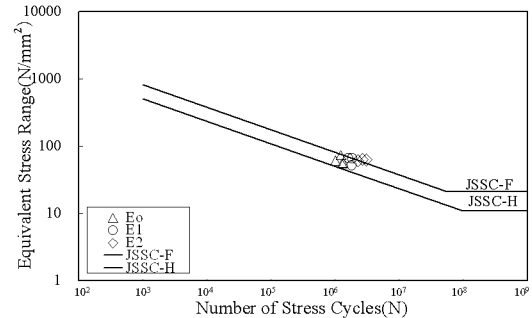


Fig. 12 S-N Curve of Tensile Grip Joints

References

- 1) Japan Society of Civil Engineers Composite Slab WG : Experimental study concerning fatigue properties of longitudinal direction joints of composite slabs.1996.3 (in Japanese)
- 2) ST. Seo, S. Hino, T. Ohta, I. Simizu: A Fundamental Study on Longitudinal Joints in Steel-Concrete Composite Slabs, Proceedings of the Japan Concrete Institute, Vol.21, No.3, 1999 (in Japanese)
- 3) S. Hino, ST. Seo, T. Ohta: Longitudinal Joint with Tensile Grip Connection and Its Design Bending Moment of Composite Slab Decks in Highway Bridges, Journal of Structural Engineering, Vol.47A, 2001.3 (in Japanese)
- 4) Japan Road Association: Specifications for Highway Bridges, 1996 (in Japanese)
- 5) Japanese Society of Steel Construction: Fatigue Design Recommendations For Steel Structures, 1995.12

(2006년 1월 20일 접수, 2006년 5월 20일 채택)